http://dx.doi.org/10.5012/bkcs.2013.34.12.3695

Structural, Electrochemical, DNA Binding and Cleavage Properties of Nickel(II) Complex $[Ni(H_2biim)_2(H_2O)_2]^{2+}$ of 2,2'-Biimidazole

Arumugam Jayamani, Vijayan Thamilarasan, Venketasan Ganesan,† and Nallathambi Sengottuvelan*

*DDE, Chemistry, Alagappa University, Karaikudi -630 003, Tami Nadu, India. *E-mail: nsvelan1975@yahoo.com*
†Acme ProGen Biotech (India) Pvt. Ltd., Salem 636 004
Received July 11, 2013, Accepted September 21, 2013

A nickel(II) complex $[Ni(H_2biim)_2(H_2O)_2](ClO_4)_2 \cdot H_2O$ (**1**) of biimidazole ligand has been synthesized and characterized (Where H_2biim = 2,2'-biimidazole). The single crystal X-ray diffraction of the complex shows a dimeric structure with six coordinated psudo-octahedral geometry. The cyclic voltammograms of complex exhibited one quasireversible reduction wave (E_{pc} = –0.61 V) and an irreversible oxidation wave (E_{pa} = 1.28 V) in DMF solution. The interaction of the complex with Calf-Thymus DNA (CT-DNA) has been investigated by absorption and fluorescence spectroscopy. The complex is an avid DNA binder with a binding constant value of 1.03×10^5 M^{-1}. The results suggest that the nickel(II) complex bind to CT-DNA *via* intercalative mode and can quench the fluorescence intensity of EB bind to CT-DNA with K_{app} value of 3.2×10^5 M^{-1}. The complex also shown efficient oxidative cleavage of supercoiled pBR322 DNA in the presence of hydrogen peroxide as oxidizing agent. The DNA cleavage by complex in presence of quenchers; *viz*. DMSO, KI, NaN_3 and EDTA reveals that hydroxyl radical or singlet oxygen mechanism is involved. The complex showed invitro antimicrobial activity against four bacteria and two fungi. The antimicrobial activity was nearer to that of standard drugs and greater than that of the free ligand.

Key Words : Nickel(II) complex, Electrochemical studies, DNA binding and cleavage studies, Anti-microbial activity

Introduction

In recent years, many researchers have focused on interaction of small molecules with Deoxyribonucleic acid (DNA).[1-3] The interaction between small molecules and DNA can cause DNA damage in cancer cells, blocking the division of cancer cells and resulting in cell death.[4,5] The cleavage of nucleic acids may be considered as an enzymatic reaction which comprises of various biological processes as well as the biotechnological manipulation of genetic material. The application of artificial DNA cleaving agents is manifold: biotechnology, structural studies of nucleic acids, or development of new drug.[6,7] Compounds showing the property of effective binding as well as cleaving double stranded DNA under physiological conditions are of importance since these could be used as diagnostic agents in medicinal and genomic research.[8] The metal complexes interact in a non-covalent fashion with DNA by intercalation, groove-face binding or external electrostatic interaction. The changes in the intensities of electronic spectra can be used to explain the nature and strength of the stacking interactions between chromophores and DNA base pairs. Of various metal complexes, the coordination behaviour of transition metal ions to different types of ligands has different properties which lead to drastic developments in various fields. The transition metal complexes are of paramount importance for designing chemotherapeutic drugs, regulating gene expression and designing tools for molecular biology from the studies on the chemical modification of nucleic acids[9-11] in which nickel is a metal which can be able to catalyze oxidative damage to nucleic acids. 2,2'-Biimidazole is an interesting ligand because of its two N sites and two –NH sites. Both N-donors are having stronger coordination ability and flexible coordination modes towards transition metals. Moreover, two –NH donors can interact with other hydrogen bonding acceptors *via* hydrogen bonds[12] and can be regarded as a robust heteromeric hydrogen-bonded synthon. The presence of an imidazole moiety in biological molecules has encouraged the studies of H_2biim containing transition metal complexes.[13,14]

Experimental

All the chemicals used for synthesis were of analytical grade and were used as received without any further purification. CT-DNA and pBR322 DNA were purchased from Sigma. Tris-HCl, Tris-base and NaCl were purchased from Merck. The electronic spectrum of the complex was recorded on a Shimadzu UV-3101PC spectrophotometer. FT-IR spectrum was recorded in the 4000-400 cm^{-1} region using KBr pellets on a Bruker EQUINOX 55 spectrometer. Elemental analysis was carried out on an Elementar vario MACRO cube elemental analyzer. A Biologic CHI604D electrochemical analyzer was used for studying the electrochemical behavior of complex using a three-electrode cell in which a glassy carbon electrode was the working electrode, a saturated Ag/AgCl electrode was the reference electrode and a platinum wire was used as an auxiliary electrode in nitrogen atmosphere. The concentration of complex was 10^{-3}

M in DMF and tetra(*n*-butyl)ammonium perchlorate (TBAP) (10^{-1} M) was used as the supporting electrolyte. (Perchlorate salts of metal complexes are potentially explosive and should be handled with care).

Synthesis of Complex (1). To a solution of $Ni(ClO_4)_2 \cdot 6H_2O$ (0.69 g, 1.85 mM) in 10 mL of methanol, biimidazole (0.50 g, 3.7 mM) in methanol (10 mL) was slowly added in drop wise with constant stirring. The mixture was stirred well at room temperature for about 3 h, the formed bluish-green solution was then concentrated to one third of its volume, washed well (with water, methanol and ether) and dried under vacuum. The complex was then recrystallized in ethanol by slow evaporation method to obtain X-ray quality single crystals of complex, which appeared gradually after several days. Yield: 0.27 g (53%). Anal. $C_{12}H_{14}Cl_2N_8NiO_{11}$: Calcd. C, 25.03; H, 2.45; N, 19.46%. Found: C, 24.88; H, 2.25; N, 19.38%. λ_{max}, (ε, M^{-1} cm^{-1}) in DMF: 1013 (10), 960 (20) 593 (25), 273 (11600), 255 nm (5450): IR (KBr pellet): 3433 (νH_2O); 3189 (νN-H); 1625 (νC=C); 1315 (νN-H); 1089 (νClO_4); 626 $\nu(ClO_4)$; 490 cm^{-1} (νNi-N).

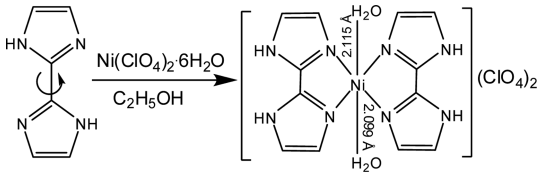

General Synthetic Route of Ni(II) Complex

X-ray Diffraction Analysis. Bluish green crystals of the complex suitable for X-ray diffraction studies were obtained from slow evaporation of ethanol solution, after standing for several days. The X-ray diffraction analysis of the complex was performed on Bruker SMART APEX-II CCD diffractometer using graphite monochromated MoKα radiation (0.71037 Å). The structure was solved using the direct methods and all non-hydrogen atoms were refined anisotrophically by full-matrix least-square procedures (SHELX97). Hydrogen atoms were added theoretically and refined with riding model position parameters and fixed isotropic thermal parameters.

DNA Binding Studies. The binding of CT-DNA with synthesized nickel(II) complex was studied using the UV absorption spectral method. The stock solution of calf thymus was prepared in 5 mM Tris-HCl/20 mM NaCl buffer (pH = 7.2), stored at 4 °C. The solution of CT-DNA gave a ratio of UV absorbance at 260 nm and 280 nm, A_{260}/A_{280}, of 1.8-1.9, indicating that the CT-DNA was sufficiently free of proteins. The concentration of DNA was determined by the UV absorbance at 260 nm after 1:100 dilutions with a molar extinction coefficient of 6600 $M^{-1}cm^{-1}$. Absorption titration experiments were made using different concentration of DNA, while keeping the complex concentration as constant. Stock solutions were stored at 4 °C and used within 4 days. Double distilled water was used to prepare all buffer solutions.

EB emits intense fluoresence in the presence of CT-DNA due to its strong intercalation between the adjacent CT-DNA base pairs. It was previously reported that the enhanced fluorescence can be quenched by the addition of a second molecule. The fluorescence spectral method using ethidium bromide (EB) as a reference was used to determine the relative DNA binding properties of the Ni(II) complex **1** to CT-DNA in 5 mM Tris–HCl/5 mM NaCl buffer, pH 7.5). Fluorescence intensities of EB at 600 nm with an excitation wavelength of 509 nm were measured at different complex concentrations. Reduction in the emission intensity was observed with addition of the complexes. The relative binding tendency of the complexes to CT-DNA was determined from a comparison of the slopes of the lines in the fluorescence intensity *vs*. complex concentration plot. The apparent binding constant (K_{app}) was calculated using the equation $K_{EB}[EB]/K_{app}[complex]$, where the complex concentration was the value at a 50% reduction of the fluorescence intensity of EB and $K_{EB} = 1.0 \times 10^7$ M^{-1} ([EB] = 3.3 μM).

DNA Cleavage Experiments. The DNA cleavage studies were done by gel electrophoresis experiment for which pBR322 was used as the plasmid DNA. DNA cleavage activity was evaluated by monitoring the conversion of supercoiled plasmid DNA (Sc – form I) to nicked circular DNA (Nick- form II) and linear DNA (Lin – form III). Each reaction mixture was prepared by adding 2 μL (200 ng) of supercoiled DNA, 2 μL of 500 mM Tris- HCl/500 mM NaCl buffer (pH = 7.4), 4 μL of hydrogen peroxide and 6 μL of the complex dissolved in DMF. The final reaction volume was 20 μL, the final buffer concentration was 50 mM and the final concentration of complex varied from 100 to 200 μM. Samples were typically incubated for 1 h at 37 ºC. After incubation, 5 μL of DNA loading buffer (0.25% bromophenol blue, 0.25% xylene cyanol, 30% glycerol in water) were added to each tube and the sample was loaded onto a 0.8% agarose gel in TBE buffer (89 mM Tris 89 mM borate, 1 mM EDTA pH 8.4) containing ethidium bromide (0.5 μg/mL). Negative and positive controls were loaded on each gel electrophoresis and the experiment was carried out for 1.30 h at 50 V. The reaction was also carried out in the same buffer but in the presence of hydrogen peroxide scavenger KI (40 mM), hydroxy radical scavenger DMSO (40 mM), singlet oxygen scavenger NaN_3(40 mM) and chelating agent EDTA (100 mM).

Antimicrobial Studies. The antimicrobial activity of the biimidazole ligand and its nickel(II) complex were tested against the bacterial species (*Staphylococcus aureus*, *Escherichia coli*, *Bacillus subtilis* and *Pseudomonas aeruginosa*) on nutrient agar medium and against the fungal species (*Aspergillus niger* and *Candida albicans*) cultured on potato dextrose agar medium by disc diffusion method. For the investigation of the antimicrobial activity, the ligand and its complex was dissolved in dimethylsulfoxide (DMSO) to a final concentration of 100 μg/mL. The sample was filled into the sterilized discs of agar plates directly, incubated at 37 ºC for 24 h for bacteria and 38 h for fungi. The diameter of inhibition zone around each disc was measured after incubation period and studies were performed in duplicate. Solvent control test was also performed in order to study the

effect of DMSO (solvent) on the growth of microorganism and it did not inhibit growth.

Results and Discussion

General Characterizations. The complex obtained in 52% yield was air-stable and characterized by elemental analysis, FT-IR and UV-vis spectral analysis. The FTIR spectrum of the complex showed broad band at 3433 cm^{-1} indicating the presence of water molecules in the complex. Weak band at 3189 cm^{-1} may be due to N-H stretching vibrations and a sharp band at 1315 cm^{-1} was attributed to N-H bending vibration. The complex showed strong bands at 1089 cm^{-1} and 626 cm^{-1} possibly due to the antisymmetric stretch and antisymmetric bend of perchlorate ions.[15] The Ni-N coordination was also confirmed by the band at 490 cm^{-1}.[16]

The electronic absorption spectrum of the complex exhibit distinct bands at 1013 nm, 960 nm and 593 nm assigned to $^3T_{2g} \leftarrow {}^3A_{2g}$, $^3T_{1g}(F) \leftarrow {}^3A_{2g}$ and $^3T_{1g}(P) \leftarrow {}^3A_{2g}$ transition of high spin pseudo-octahedral Ni(II) complex, respectively.[17] The sharp intense peaks at 270 and 255 nm were attributed to the π–π^* transitions of biimidazole ligand. The electronic spectrum of the synthesized nickel(II) complex is in very good agreement with the previously reported pseudo-octahedral geometry of the complexes.[18,19]

Crystal Structure. The ORTEP diagram of nickel(II) complex is shown in Figure 1. The crystallographic data is listed in Table 1 and selected bond distances and bond angle are given in Table 2. Single crystal X-ray diffraction analysis showed that the complex $[Ni(H_2biim)_2(H_2O)_2](ClO_4)_2{\cdot}H_2O$ crystallizes as triclinic crystal system with P_1 space group. Each nickel(II) atom is coordinated by two aqua and two bidentate biimidazole ligands, resulting in a slightly distorted octahedral NiN_4O_2 coordination geometry. The molecular structure contained two different molecules A and B are shown in Figure 1. The four nitrogen atoms of two biimidizole ligands and two aqua atoms lie in the equatorial plane and axial sites, respectively. In molecule A, the four Ni–N bond lengths vary in the range of 2.079-2.108 Å and the aqua oxygen occupies the apical position with an elongated Ni–O bond length of 2.115 Å.

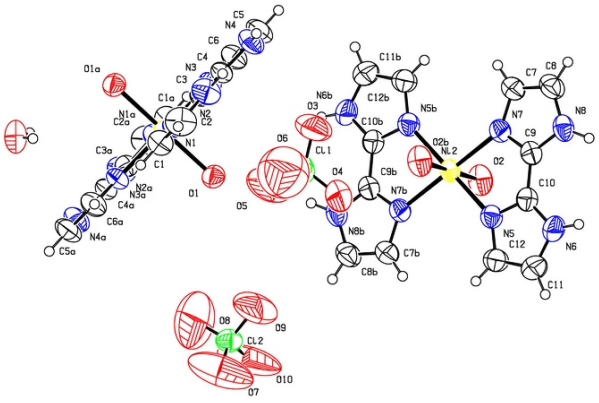

Figure 1. ORTEP view of the molecular structure of complex.

Table 1. Crystallographic data and structure refinement parameters for the complex (**1**)

Complex	**1**
chemical formula	$C_{12}H_{14}Cl_2N_8NiO_{11}$
Fw	575.9
Crystal system	triclinic
Space group	$P\bar{1}$
a/Å	7.878(4)
b/Å	11.123(4)
c/Å	13.227(6)
α/deg	84.92(2)
β/deg	88.86(2)
γ/deg	79.31(1)
V/Å^3	1134.45(9)
Z	2
completeness	97.5%
F(000)	584
q/deg	1.55 to 28.23
GOF (F^2)	1.019
R_1 [$I > 2\sigma(I)$]	0.065
wR_2 (all data)	0.199

The N–Ni–N bond angles vary from 80.5 to 99.6°. In molecule B, the four Ni–N bond lengths vary in the range 2.096–2.103 Å and the aqua oxygen occupies the apical position with an elongated Ni–O bond length of 2.099 Å. The N–Ni–N bond angles vary from 79.7 to 100.3°. $[Ni(H_2biim)_2(H_2O)_2]^{2+}$ with anions such as chloride and 3-methylbenzoate have been reported earlier.[20-22] Even though there are some reported complexes of biimidazole already available the nickel complex with perchlorate ion is not yet reported. The crystal structure obtained in this paper has dimeric structure and differs from those reported earlier with

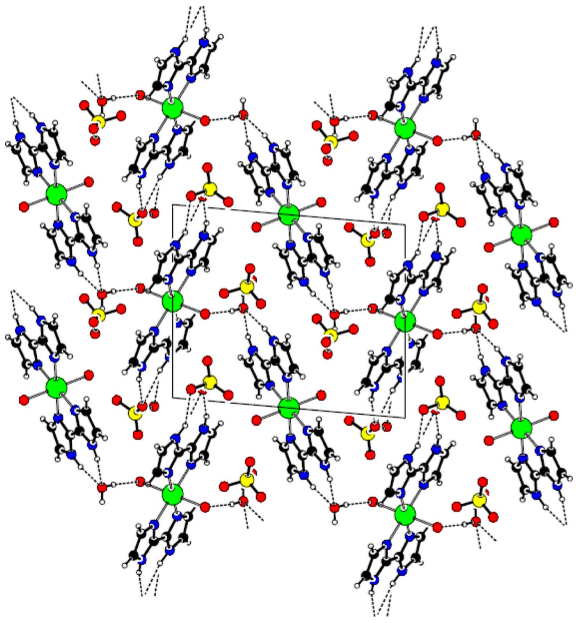

Figure 2. Crystal Packing diagram of dimeric Ni(II) complex.

different anions. The similar other aqua compounds which have common bridging coordination modes in their metal complexes such as $[Zn(H_2biim)(H_2O)_2]n$,[23] the two oxygen atoms from two H_2O molecule are in a straight line with angle of (O–Ni–O) 180° in both molecule A and B. In the crystalline state of 2,2'-biimidazole ligand, the five atoms in each ring are coplanar, but the two rings are rotated in central C-C bond and the N-H bonds are oriented in trans position. After metal binding, the two rings are rotated and N-H bonds in cis position.

Crystal structure show extensive intermolecular non-covalent interactions involving the axial aqua ligand, lattice anion and the biimidazole. One of the perchlorate anion does not only assist the packing of the complex, but also it participates in bridging of molecules A and B. Each axially coordinated oxygen atom form three hydrogen bonds with the two perchlorate anion and one with the lattice water molecule. In addition, one of the perchlorate anion forms N2H2···O3 hydrogen bond with the biimidazole nitrogen atom. The potential hydrogen bonds involved in the structures are also given in the Table 3.The lattice water molecule form hydrogen bond with biimidazole nitrogen.[24-26] The one dimension chain is linked by the weak hydrogen-bonds formed by axially coordinated aqua hydrogen atoms bonded to perchlorate oxygen atoms. One dimension chain is extended in zigzag manner to form two-dimension network by intermolecular hydrogen-bonds (Figure 2).

The distance between Ni1 and Ni2 in the crystal packing is 9.010 Å, the angle between two Ni atoms is found to be 73.24°. This arrangement leads to zigzag arrangement of the atoms in crystal packing. The hydrogen bonding interactions gives rise to a two dimensional network having well-defined channels. We thus consider that many hydrogen bonding interaction stabilize the molecules and plays an important role in the formation of this chains structure.

Table 2. Selected bond lengths (Å) and bond angles (°) for the complex (**1**)

Bond distances	(Å)	Bond angles	(°)
Ni(2)-N(5)	2.096(4)	N(5)-Ni(2)-O(2)	88.30(2)
Ni(2)-N(5)#1	2.096(4)	N(5)-Ni(2)-N(7)#1	100.26(1)
Ni(2)-O(2)#1	2.099(3)	O(2)-Ni(2)-N(7)#1	88.18(1)
Ni(2)-O(2)	2.099(3)	N(5)-Ni(2)-N(7)	79.74(1)
Ni(2)-N(7)#1	2.104(3)	O(2)-Ni(2)-N(7)	91.82(1)
Ni(2)-N(7)	2.104(3)	N(3)-Ni(1)-N(1)	80.44(1)
Ni(1)-N(3)#2	2.079(3)	N(3)-Ni(1)-N(1)#2	99.56(1)
Ni(1)-N(3)	2.079(3)	N(1)-Ni(1)-O(1)#2	87.63(1)
Ni(1)-N(1)	2.107(3)	N(3)#2-Ni(1)-O(1)	91.32(1)
Ni(1)-N(1)#2	2.107(3)	N(3)-Ni(1)-O(1)	88.68(1)
Ni(1)-O(1)#2	2.115(3)	N(1)-Ni(1)-O(1)	92.37(1)
Ni(1)-O(1)	2.115(3)	N(1)#2-Ni(1)-O(1)	87.63(1)
N(5)-C(10)	1.315(5)	C(3)-N(1)-Ni(1)	110.9(3)
N(5)-C(12)	1.375(6)	C(1)-N(1)-Ni(1)	143.1(3)
N(6)-C(10)	1.325(6)		
N(7)-C(9)	1.311(6)		
N(6)-C(11)	1.363(7)		
N(8)-C(9)	1.337(5)		
N(8)-C(8)	1.375(7)		
N(7)-C(7)	1.375(6)		

Table 3. Hydrogen bonds for the complex (**1**)

D-H···A	d(D-H) (Å)	d(H···A) (Å)	d(D···A) (Å)	<(DHA) (°)
N(2)-H(2)···O(3)#1	0.86(5)	2.104(9)	2.93(1)	161.4(4)
N(4)-H(4)···O(6)#1	0.93(7)	2.42(8)	3.15(2)	135(6)
N(4)-H(4)···Cl(1)#2	0.93(7)	2.86(8)	3.756(5)	164(6)
C(6)-H(6)···O(10)#3	0.931(5)	2.443(8)	3.31(1)	155.6(4)
C(7)-H(7)···O(9)#4	0.931(5)	2.66(1)	3.24(1)	121.6(4)
N(6)-H(6)···O(1S)#5	0.86(5)	2.102(5)	2.892(7)	152.5(3)
N(8)-H(8)···O(1S)#5	0.89(5)	2.05(5)	2.891(6)	155(5)

Symmetry transformations used to generate equivalent atoms: #1 x, −1+y, z. #2 2−x, 2−y, −z. #3 2−x, 1−y, 1−z. #4 2−x, 2−y, 1−z. #5 1−x, 1−y, −z

Electrochemistry. The complex showed metal-centered quasi-reversible cyclic voltammetric response due to the Ni(II)/Ni(I) couple near −0.61 V versus Ag/AgCl in DMF containing 0.1 M TBAP (Figure 3). The ligand-centered cyclic voltammetric responses were observed at −1.29 V.

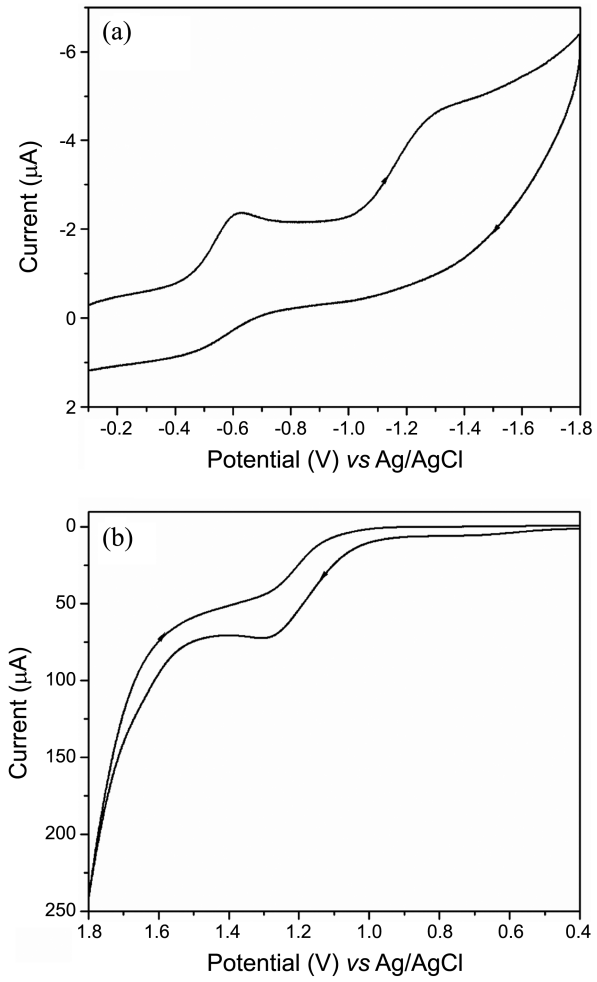

Figure 3. Cyclic voltammogram of **1** (a) Reduction process & (b) Oxidation process.

The separation of the anodic and cathodic peak potential is 190 mV, and the ratio of anodic to cathodic peak currents, $i_{pa}/i_{pc} = 1.43$, indicating a quasi-reversible redox process. One quasi-reversible oxidation wave was observed at $E_{pa} = 1.28$ V can be assigned to the redox couple[27] of Ni(II)/Ni(III). The obtained redox behavior of the complex is similar to that of already reported NiN_4 complexes.[28-30]

DNA Binding Studies. To investigate the mode of binding between the complex and the DNA double helix, absorption studies and fluorescence spectroscopic studies were carried out. Absorption titration experiments with CT-DNA show intense absorption peaks at 245 and 280 nm in the UV region of the complex that could be attributed to intraligand $\pi \rightarrow \pi^*$ transition of the coordinated groups in the complex. On addition of increasing amounts of DNA to the complex, both of the two characteristic peaks decreased gradually with the maximum hypochromicity of 15% and 20%, respectively, suggesting the strong interaction between complex and DNA. The absorption peak at 280 nm shifts towards lower wavelength with the increase of DNA concentration, *i.e* an obvious bathochromism (~2-3 nm) was found, which demonstrated that the complex probably bind to DNA *via* an groove binding mode.[31]

The spectrophotometric titration of the complex is shown in Figure 4. In order to calculate quantitatively the binding strength of the complex, the intrinsic binding constant (K_b) value of the complex with CT-DNA was determined according to the following equation[32]

$$[DNA]/(\varepsilon_a - \varepsilon_f) = [DNA]/(\varepsilon_b - \varepsilon_f) + 1/K_b\,(\varepsilon_b - \varepsilon_f)$$

where [DNA] is the concentration of DNA in base pairs, the apparent absorption coefficients ε_a, ε_f and ε_b correspond to A_{obsd}/[complex], the extinction coefficient for the free complex and the extinction coefficient for the complex in the fully bound form, respectively. In plots of $[DNA]/(\varepsilon_b - \varepsilon_f)$ versus [DNA], K_b is given by the ratio of the slope to the intercept. The K_b value obtained from the absorption spectral technique for the complex was calculated as $1.03 \times 10^5\ M^{-1}$ which is relevant to that of other typical intercalators.[33] The

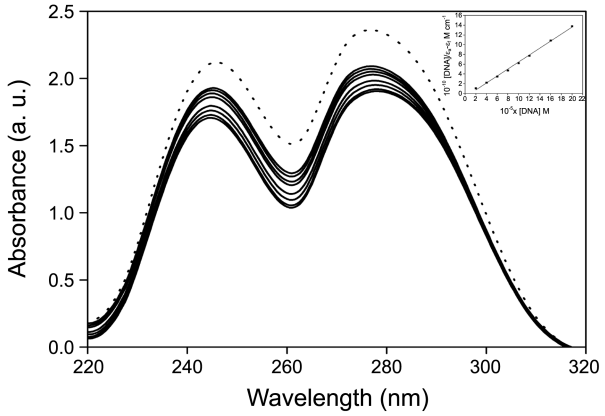

Figure 4. Absorption spectrum of **1** (40 μM) in 5 mM Tris-HCl/ 20mM NaCl buffer at pH 7.2 in the absence and presence of increasing amounts of DNA. Inset shows the least-squares fit of $[DNA]/\varepsilon_a$-ε_f *vs*. [DNA] for the complex.

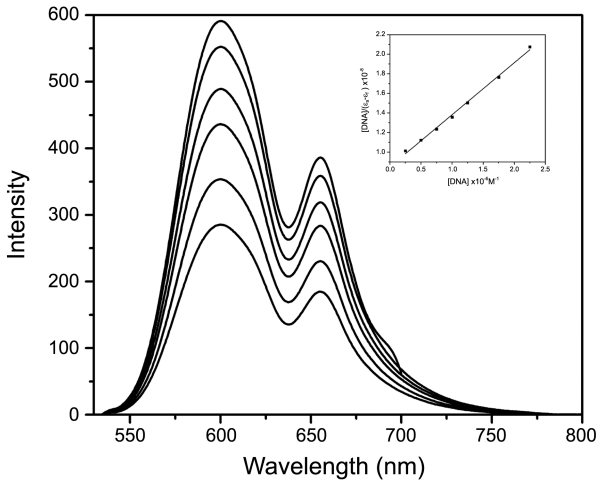

Figure 5. Emission spectrum of EB bound to DNA in the presence of complex **1** ([EB] = 3.3 μM, [DNA] = 40 μM, [complex] = 0-25 μM, K_{ex} = 510 nm). Inset shows the plots of emission intensity I_0/I *vs*. [DNA]/[complex].

strong DNA binding nature of the complex may be due to the $\pi-\pi^*$ interactions through the heterocyclic ring of the nitrogen bases. The fluorescence spectra of ethidium bromide (EB) were measured using an excitation wavelength of 509 nm and the emission range was set between 590 and 650 nm were measured with different concentrations of the complex. The emission spectrum of the EB-bound to DNA in the absence and presence of variable concentrations of the complex is shown in Figure 5. The fluorescence quenching of EB bound to DNA by the complex is in good agreement with the classical linear Stern–Volmer equation[34]

$$I_0/I = 1 + K_{sv}[Q]$$

Where, I_0 and I are the emission intensity in the absence and presence of the complex. K_{sv} is the linear Stern–Volmer quenching constant and Q is the ratio of the total concentration of the complex to that of DNA.

The K_{sv} value for the complex was found to be 1.98×10^4 M^{-1} which is given by the slope to y-intercept value from the plot of I_0/I versus [Q]. The apparent binding constant (K_{app}) was also calculated by the equation,

$$K_{EB}[EB] = K_{app}[Complex]$$

Where the concentration of the complex was determined by the value at a 50% reduction of the fluorescence intensity of EB and $K_{EB} = 1 \times 10^7\ M^{-1}$ ([EB] = 0.96×10^{-4} M). Ethidium bromide emits an intense fluorescent light when intercalated between two DNA base pairs. In presence of an additional DNA binding molecule, the emission of the DNA-EB adduct is quenched, either by replacing the EB and or by accepting the excited state electron of the EB through a photoelectron transfer mechanism.[35] A reduction in emission intensity was observed, indicating that the complex binds to the DNA helix. The apparent association constant (K_{app}) value was measured to be $3.2 \times 10^5\ M^{-1}$ for the Ni(II) complex. The binding constant value obtained for the present nickel(II) complex is similar to that of other mixed

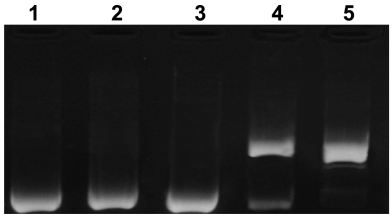

Figure 6. Cleavage of SC pBR322 DNA (0.2 μg, 33.3 μM) by **1** in the presence H_2O_2 (200 μM) as oxidizing agent in 50 mM Tris–HCl/50 mM NaCl buffer (pH 7.2). Lane 1, DNA control; lane 2, DNA + H_2O_2; lane 3, DNA + **1** (200 μM); lane 4, DNA + H_2O_2 + **1** (100 μM); lane 5, DNA + H_2O_2 + **1** (200 μM).

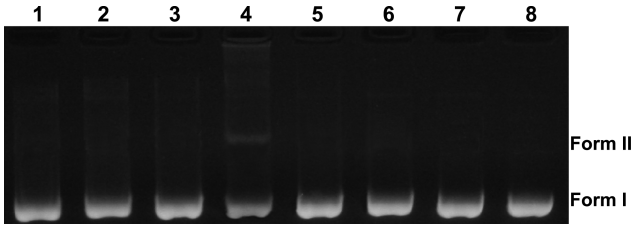

Figure 7. Cleavage of SC pBR322 DNA (0.2 μg, 33.3 μM) by Ni(II) complex **1** (100 μM) in the presence of hydroxyl radical scavengers (DMSO – 40 mM, KI – 40 mM), singlet oxygen scavenger (NaN_3 – 40 mM) and Chelating agent (EDTA – 0.1 M) in 50 mM Tris–HCl/50 mM NaCl buffer (pH 7.2). Lane 1, DNA + H_2O_2 + DMSO; Lane 2, DNA + H_2O_2 + DMSO + **1**; Lane 3, DNA + H_2O_2 + KI; Lane 4, DNA + H_2O_2 + KI + **1**; Lane 5, DNA + H_2O_2 + NaN_3; Lane 6, DNA + H_2O_2 + NaN_3 + **1**; Lane 7, DNA + H_2O_2 + EDTA; Lane 8, DNA + H_2O_2+ EDTA + **1**.

ligand biimidazole complexes[36] and substituted biimidazole complexes[37] which reveals that the synthesized nickel(II) complex having good binding propensity.

DNA Cleavage Studies. The DNA cleavage activity of the complex was investigated by agarose gel electrophoresis. Figure 6 shows the results of the gel electrophoresis separations of plasmid pBR322 DNA by the complex in the presence of H_2O_2 as an oxidizing agent. The cleavage activity was assessed by the conversion of supercoiled DNA (Form I) to its nicked (Form II) and linear (Form III) forms. As observed in lanes 1-3, DNA, H_2O_2 and complex do not induce obvious cleavage individually, when complex coexists with H_2O_2 (lane 4), a prominent DNA scission is observed. More than 60% of DNA is converted from Form I to Form II by the complex at 100 μM. The conversion from Form I to Form II and Form III is found maximum at 200 μM concentration of complex (lane 5). The cleavage ability of the complex might be due to the presence of Ni^{2+} ions which can promote the probability of double strand scission immediately after the DNA has undergone a single strand break. It is evident that the complex showed significant cleavage activity in the presence of the oxidant. This may be attributed to the formation of hydroxyl free radicals, which oxidized Ni(II) to Ni(III), which in turn could give cause for oxidative damage of DNA.[38]

In order to establish the DNA cleavage mechanism of the synthesized complex, the cleavage of DNA was further investigated both in the presence and absence of scavengers of oxidative species. Oxidative cleavage of plasmid DNA species may lead to the formation of hydrogen peroxide (H_2O_2), and/or hydroxyl radical (HO•) species, which cause damage to the sugar and/or base. To reveal the DNA cleavage mechanism, hydrogen peroxide scavenger (KI), hydroxyl radical scavenger (DMSO), singlet oxygen scavenger (NaN_3) and chelating agent (EDTA) were used[39] and the results are illustrated in Figure 7.

In the experiment for the cleavage of DNA by **1**, no significant cleavage was observed in the presence of DMSO (lane 2) and KI (lane 4) indicating that hydroxyl radical involved in the cleavage process. The addition of sodium azide (singlet oxygen quencher) also inhibits the cleavage process (lane 6) indicating that $^1O_2$ is the activated oxygen intermediate responsible for the cleavage and the chelating agent also inhibit the cleavage process (lane 8) of Ni(II) complex. When the cleavage mechanism was compared with similar reported complex[40] $[Cu(bpy)_2]^{2+}$ which cleaves by super oxide radical and in our case the cleavage occurs due to hydroxyl radical through Fenton type reactions and there is some effect of singlet oxygen. Superoxide radical generated from molecular oxygen *via* an electron transfer step which causes DNA cleavage by guanine oxidation, in case of nickel(II) complex singlet oxygen only modifies the guanine residues. The singlet oxygen might form as a result of hydrogen peroxide reacting[41,42] with O_2 coordinated with Ni atom in the complex. The significant increase in the DNA cleavage activity by **1** in the presence of H_2O_2 and the inhibition of activity in the presence of DMSO, KI, NaN_3 and EDTA suggest that this reaction was preferentially proceeded by a hydroxyl radical mechanism with •OH and

Table 4. Antimicrobial activity of the ligand and its Ni(II) complex (**1**)

Compound	Zone Inhibition Diameter (mm)					
	Bacterium				Fungi	
	Gram negative		Gram positive			
	E. coli	*P. aeruginosa*	*B. subtilis*	*S. aureus*	*A. niger*	*C. albicans*
2,2'-biimidazole	6	7	8	8	6	9
Ni(II) Complex	14	15	15	16	12	13
Amikacin	18	18	18	18	NT	NT
Ketokonazole	NT	NT	NT	NT	19	19

NT- Not tested

singlet oxygen species.

Antimicrobial Studies. The ligand and its nickel(II) complex were tested against four pathogenic bacteria and two fungi to evaluate their efficacy as antimicrobial agents. The zone of inhibition values for the antimicrobial activity was given in Table 4. The results revealed that the nickel(II) complex has higher antimicrobial activity than the free ligand which can be explained on the basis of chelation theory.[32,43] The chelation reduces the polarity of ligand due to the overlap of the ligand orbital and partial sharing of the positive charge of the nickel ion with donor groups. Further, it increases the delocalization of π-electrons over the whole chelate ring and enhances the lipophilic nature of the complex. This increased lipophilicity enhances the transportation of the complex into lipid membrane and restricts further multiplicity of the microorganisms. The obtained results using the complex have also been compared with those of the standard drugs, amikacin and ketokonazole for bacteria and fungi respectively. The complex exhibited lower activities compared with the respective standard drugs but having higher antimicrobial activity than ligand molecule.

Conclusion

In this study we have synthesized a nickel(II) complex with 2,2'-biimidazole ligand and studied their electrochemical, antimicrobial, DNA binding and oxidative DNA cleavage activities. Single crystal X-ray diffraction analysis of the synthesized Ni(II) complex confirmed a dimeric structure and molecular packing leading two dimensional network chain. The electrochemical study revealed that one reduction process occurs at negative potential and one oxidation process occurs at positive potential region. The complex showed efficient DNA binding ability and the binding constant value is consistent with other typical intercalators. The synthesized complex has significant oxidative chemical nuclease activity which could induce scission of pBR322 supercoiled DNA effectively to linear form in the presence of hydrogen peroxide as oxidizing agent and the cleavage mechanism was proceeding by a hydroxyl radical mechanism with •OH and singlet oxygen species. The antimicrobial activity of the complex was found to be greater than free ligand and nearer to the standard drugs.

Acknowledgments. The authors gratefully acknowledge the financial support of this work by the Department of Science and Technology, New Delhi (DST-SR/FT/CS-049/2009). The authors thank the STIC Cochin University of Technology, Cochin for single crystal X-ray diffraction analysis of the ligand complex. And the publication cost of this paper was supported by the Korean Chemical Society.

Supplementary Material. Crystallographic data in CIF format for the ligand and complex have been deposited at the Cambridge Crystallographic Data Centre, CCDC No. 904869 and 904868 respectively. Copies of CIFs are available free of charge from The Director, CCDC, 12 Union Road, Cambridge, CB2 1EZ, UK (fax: -/44-1223-336-033; email: deposit@ccdc.cam.ac.uk or http://www.ccdc.cam. ac.uk).

References

1. Reddy, P. R.; Shilpa, A. *Ind. J. Chem.* **2010**, *49*, 1003.
2. Kulaksizoglu, S.; Gokce, C.; Gup, R. *Turk. J. Chem.* **2012**, *36*, 717.
3. Dasgupta, D.; Majumder, P.; Banerjee, A. *J. Biosci.* **2012**, *37*, 475.
4. Vaidyanathan, V. G.; Nair, B. U. *J. Inorg. Biochem.* **2002**, *91*, 405.
5. Ye, B. H.; Ding, B. B.; Weng, Y. Q.; Chen, X. M. *Cryst. Growth Des.* **2005**, *5*, 801.
6. Ding, B. B.; Weng, Y. Q.; Mao, Z. W.; Lam, C. K.; Chen, X. M.; Ye, B. H. *Inorg. Chem.* **2005**, *44*, 8836.
7. Tadokoro, M.; Nakasuji, K. *Coord. Chem. Rev.* **2000**, *198*, 218.
8. Sang, R. L.; Zhu, M. L.; Yang, P. *Acta Cryst.* **2002**, *58*, m172.
9. Collier, H. L. *Korea polymer J*. **1997**, *5*, 179.
10. Biswas, R.; Drew, M. G. B.; Ghosh, A. *Inorg. Chem. Commun.* **2012**, *24*, 1.
11. Nakamoto, K.; In *Infrared and Raman Spectra of Inorganic and Coordination Compounds*, 4th ed.; John Wiley & Sons: New York, 1986.
12. Halcrow, M. A.; Christou, G. *Chem. Rev.* **1994**, *94*, 2421.
13. Stavropoulos, P.; Muetterties, M. C.; Carrie, M.; Holm, R. H. J. *Am. Chem. Soc.* **1991**, *113*, 8485.
14. Tucci, G. C.; Holm, R. H. *J. Am. Chem. Soc.* **1995**, *117*, 6489.
15. Mukherjee, P.; Drew, M. G. P.; Estrader, M.; Ghosh, A. *Inorg. Chem*. **2008**, *47*, 784.
16. Yang, L. F.; Cao, M. L.; Mo, H. J.; Hao, H. G.; Wu, J. J.; Zhang, J. P.; Ye, B. H. *CrystEngComm* **2009**, *11*, 1114.
17. Qiu, Q. M.; Deng, Y. H.; Sun, J. J.; Yang, W.; Jin, Q. H.; Zhang, C. L. *Z. Kristallogr.* **2011**, *226*, 625.
18. Zhang, Y.; Li, J.; Lin, W.; Liu, S.; Huang, J. *J. Crystallogr. Spectrosc. Res.* **1992**, *22*, 434.
19. Angela, K.; Lucica, A. V.; Nicoleta, C.; Ileana, R.; Nicolae, S. *J. Serb. Chem. Soc.* **2011**, *75*, 229.
20. Zhong, Y. R.; Cao, M. L.; Mo, H. J.; Ye B. H. *Cryst. Growth Design* **2008**, *8*, 2282.
21. Hui, Z. *Acta Cryst.* **2009**, *E65*, m1497.
22. Mighell, A. D.; Reimann, C. W.; Mauer, F. A. *Acta Cryst.* **1969**, *B25*, 60.
23. Carranza, J.; Sletten, J.; Lloret, F.; Julve, M. *Polyhedron* **2009**, *28*, 2249.
24. Wang, Q. W.; Xu, Y. Y.; Xu, Z.-L.; Wang, J. J. *Z. Kristallogr.* **2009**, *224*, 157.
25. Akkawi, M.; Aljazzar, A.; Haj, M. A.; Remeleh, Q. A. *Br. J. Pharmacol. Toxicol*. **2012**, *3*, 65.
26. Bu, X. H.; Zhang, Z. H.; Cao, X. C.; Zhu, Z. A.; Chen, Y. T. *Trans. Met. Chem.* **1997**, *22*, 1.
27. Grochala, W.; Jagielska, A.; Wozniak, K.; Wieckowska, A., Bilewicz, R.; Daszkiewicz, B. K.; Bukowska, J.; Piela, L. *J. Phys. Org. Chem.* **2001**, *14*, 63.
28. Choi, K. Y.; Kim, M. J.; Kim, D. S.; Kim, Y. S.; Kim, J. H.; Ryu, H.; Lim, Y. M.; Kang, S. G.; Shin, U. S.; Lee, K. C.; Hong, C. P. *Bull. Korean Chem. Soc.* **2002**, *23*, 1062.
29. Choi, K. Y.; Lee, H. H.; Park, B. B.; Kim, J. H.; Kim, J.; Kim, M. W.; Ryu, J. W.; Suh, M.; Suh, I. H. *Polyhedron* **2001**, *20*, 2003.
30. Khan, S.; Nami, S. A. A.; Siddiqi, K. S.; Husain, E.; Naseem, I. *Spectrochim. Acta Part A* **2009**, *72*, 421.
31. Li, Y.; Wu, Y.; Zhao, J.; Yang, P. *J. Inorg. Biochem.* **2007**, *101*, 283.
32. Peng, B.; Chao, H.; Sun, B.; Li, H.; Gao, F.; Ji, L. N. *Inorg. Biochem.* **2006**, *100*, 1487.
33. Nair, R. B.; Teng, E. S.; Kirkland, S. L.; Murphy, C. J. *Inorg. Chem.* **1998**, *37*, 139.
34. Dong, X.; Wang, X.; Lin, M.; Sun, H.; Yang, X.; Guo, Z. *Inorg. Chem.* **2010**, *49*, 2541.

35. Lakowicz, J. R.; Weber, G. *Biochemistry* **1973**, *12*, 4161.
36. Nagasubramanian, S.; Thamilarasan, V.; Jayamani, A.; Kang, S. K.; Kim, Y.-I.; Sengottuvelan, N. *Bull. Korean Chem. Soc.* **2013**, *34*, 1875.
37. Li, Y.; Wu, Y.; Zhao, J.; Yang, P. *J. Inorg. Biochem.* **2007**, *101*, 283.
38. Baguley, B. C.; Bret, M. L. *Biochemistry* **1984**, *23*, 937.
39. Srivastava, R. S. *Inorg. Chim. Acta* **1981**, *56*, 65.
40. Park, K.-J.; Kwon, J. H.; Cho, T.-S., Kim, J. M.; Hwang, I. H.; Kim, C.; Kim, S.; Kim, J.; Kim, S. K. *J. Inorg. Biochem.* **2013**, *127*, 46.
41. Ryter, S. W.; Tyrrell, R. M. *Free Radic. Biol. Med.* **1998**, *24*, 1520.
42. Kim, J. M.; Kim, S. K. *Bull. Korean Chem. Soc.* **2011**, *32*, 3.
43. Joseyphus, R. S.; Nair, M. S. *Mycobiol.* **2008**, *36*, 93.